Inorg. Chem. **2004**, *43*, 8404–8413

Bicyclic and Acyclic Diamides: Comparison of Their Aqueous Phase Binding Constants with Nd(III), Am(III), Pu(IV), Np(V), Pu(VI), and U(VI)

Serguei I. Sinkov,* Brian M. Rapko, Gregg J. Lumetta, and Benjamin P. Hay

Pacific Northwest National Laboratory, Richland, Washington 99352

James E. Hutchison and Bevin W. Parks

Department of Chemistry, University of Oregon, Eugene, Oregon 97403

Received May 12, 2004

This report describes affinity measurements for two, water-soluble, methyl-alkylated diamides incorporating the malonamide functionality, *N*,*N*,*N*′,*N*′ tetramethylmalonamide (TMMA) and a bicyclic diamide (**1a**), toward actinide metal cations (An) in acidic nitrate solutions. Ligand complexation to actinides possessing oxidation states ranging from +3 to +6 was monitored through optical absorbance spectroscopy, and formation constants were obtained from the refinement of the spectrophotometric titration data sets. Species analysis gives evidence for the formation of 1, 4, 1, and 2 spectrophotometrically observable complexes by TMMA to An(III, IV, V, and VI), respectively, while for **1a**, the respective numbers are 3, 4, 2, and 2. Consistent with the preorganization of **1a** toward actinide binding, a significant difference is found in the magnitudes of their respective formation constants at each complexation step. It has been found that the binding affinity for TMMA follows the well-established order An(V) < An(III) < An(VI) < An(IV). However, with **1a**, Np(V) forms stronger complexes than Am(III). The complexation of **1a** with Np(V) and Pu(VI) at an acidity of 1.0 M is followed by reduction to Np(IV) and Pu(IV), whereas TMMA does not perturb the initial oxidation state for these dioxocations. These measurements of diamide binding affinity mark the first time single-component optical absorbance spectra have been reported for a span of actinide–diamide complexes covering all common oxidation states in aqueous solution.

1. Introduction

Diamides have been studied extensively as agents for the selective extraction of trivalent f-block metal ions from aqueous solutions.[1−4] They form the basis for separation processes designed to partition the minor actinides from spent nuclear fuel for subsequent transmutation (with concomitant closure of the nuclear fuel cycle) or immobilization (for disposal). One drawback associated with the current generation of diamide extractants is the relatively modest actinide distribution coefficients obtained even at high (>1.0 M) extractant concentrations. Recently, we described the extraction characteristics for a new type of diamide molecule that we believe to be well organized for complexation to f-block metal cations.[5,6] This new diamide (as Structure **1b**, Figure 1) exhibited a 10^6 to 10^7 enhancement over

previously examined diamides (e.g., *N*,*N*,*N*′,*N*′-tetraalkylmalonamides) in the extraction of trivalent lanthanides and actinides from aqueous solution. Furthermore, in these previous studies the chemistry of f-element metal ions in other oxidation states was not explored.

In these earlier reports, it was assumed that the observed extraction enhancement reflected a superior ligand−metal binding of the bicyclic diamide as compared to acyclic

* To whom correspondence should be addressed. E-mail: serguei.sinkov@pnl.gov.

(1) Mathur, J. N.; Murali, M. S.; Nash, K. L. *Solvent Extr. Ion Exch.* **2001**, *19* (3), 357−390.
(2) Charbonnel, M. C.; Flandin, J. L.; Giroux, S.; Presson, M. T.; Madic, C.; Morel, J. P. In *Proceedings of the International Solvent Extraction Conference, ISEC-2002*; 2002; pp 1154−1160.
(3) Spjuth, L.; Liljenzin, J. O.; Skalberg, M.; Hudson, M. J.; Chan, G. Y. S.; Drew, M. G. B.; Feaviour, M.; Iveson, P. B.; Madic, C. *Radiochim. Acta* **1997**, *78*, 39−46.
(4) Sasaki, Y.; Tachimori, S. *Solvent Extr. Ion Exch.* **2002**, *20* (1), 21−34.
(5) Lumetta, G. J.; Rapko, B. M.; Garza, P. A.; Hay, B. P.; Gilbertson, R. D.; Weakley, T. J. R.; Hutchison, J. E. *J. Am. Chem. Soc.* **2002**, *124*, 5644−5645.
(6) Lumetta, G. J.; Rapko, B. M.; Hay, B. P.; Garza, P. A.; Hutchison, J. E.; Gilbertson, R. D. *Solvent Extr. Ion Exch.* **2003**, *21*, 29−39.

10.1021/ic049377m CCC: $27.50
Published on Web 11/25/2004

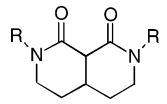

Figure 1. New optimized bicyclic diamide ligand architecture for bidentate lanthanide/actinide binding; R = methyl (**1a**), R = octyl (**1b**).

analogues such as *N*,*N*,*N*′,*N*′-tetraalkylmalonamides. However, changes in ligand−metal binding affinity as a function of changing diamide structure were not directly quantified. An understanding of the thermodynamic details behind such structure−function aspects of the actinide extraction by diamides in all common available oxidation states will be needed to intelligently design extractants with characteristics superior to those currently available.

A first step toward understanding the thermodynamic details of diamide−actinide interactions is to evaluate their binding constants in a single phase. One possible approach to quantify the magnitude of ligand-to-metal binding is the application of ultraviolet−visible (UV−vis) optical absorbance spectroscopy to monitor the spectral changes induced by **1a** in the absorption spectra of actinide ions in aqueous solution. The spectral information obtained by varying the ligand-to-metal ratio not only allows the number of light-absorbing species in solution to be estimated,[7] but also can be used to measure the binding (or formation) constants of a ligand with metal ions.[8] In this report, we describe the formation constants for the *N*,*N*′-dimethyl bicyclic diamide (**1a**) and for *N*,*N*,*N*′,*N*′-tetramethylmalonamide (TMMA) with all the common oxidation states of actinides in acidic solution: An(III), represented by Am(III) [and Nd(III) as a nonradioactive analog], An(IV) by Pu(IV), An(V) by Np(V), and An(VI) by U(VI) and Pu(VI), under the comparable aqueous conditions of 1.0 M ionic strength ($HNO_3/NaNO_3$). Our choice of nitric acid/sodium nitrate, as opposed to the more common choice $HClO_4/NaClO_4$, as ionic strength supporting electrolyte, was made to faciliate the application of the complexation data to a large body of diamide solvent extraction data of the lanthanides and actinides with various lipophilic analogues of TMMA and **1a**.

2. Experimental Section

2.1. General. TMMA was purchased from TCI America. The bicyclic diamide **1a** was prepared and characterized according to the literature.[5,9] Uranyl nitrate hexahydrate and neodymium perchlorate were obtained from commercial sources and were of reagent-grade purity or better. The radionuclides ^{243}Am, ^{237}Np, and ^{239,240}Pu were obtained from in-house stocks.

2.2. Preparation of Metal Solutions, Valency Adjustments, and Solution Standardization. *Nd(III).* An Nd working solution was produced from a standard solution of aqueous $Nd(ClO_4)_3$. The Nd concentration in the stock solution was verified by visible spectroscopy by the absorbance of the peak at 576 nm (ϵ = 7.2 M^{-1} cm^{-1}).[10]

Am(III). An Am working solution was prepared from a stock solution of ^{243}Am in 1.0 M HNO_3. The ^{243}Am concentration was determined by gamma-energy analysis and verified with visible spectroscopy by the absorbance of the peak at 811 nm (ϵ = 64.4 M^{-1} cm^{-1}).[11]

Pu(IV). The ^{239,240}Pu(IV) working solution was prepared by an 85-fold dilution of an in-house 0.68 M Pu(IV) stock solution stored in 4.0 M HNO_3 into 1.0 M nitric acid. The ^{239,240}Pu(IV) concentration in the main stock solution was determined spectrophotometrically by the absorbance of the peak at 476 nm (ϵ = 80.3 M^{-1} cm^{-1})[12] after dilution in 2.2 M HNO_3. Measurement of the visible spectrum also indicates a valence purity of greater than 99.5% in the working solution.

Np(V). A ^{237}Np(V) working solution was prepared by digesting a Np(IV, V, and VI) stock solution in concentrated nitric acid followed by complete evaporation of the liquid, dissolution of the residue in 1.0 M HNO_3, and careful reduction of Np(VI) by a controlled amount of hydrazine nitrate. The ^{237}Np concentration was determined by γ-spectroscopy, and visible spectroscopy indicated that a valence purity of greater than 99% was achieved.

U(VI). A U(VI) working solution was prepared by dissolution of $UO_2(NO_3)_2 \cdot 6H_2O$ in 1.0 M HNO_3. The uranium concentration in solution was determined by visible spectroscopy using the optical absorbance band intensity at 414.1 nm (ϵ = 8.3 M^{-1} cm^{-1}, unpublished data).

Pu(VI). A Pu(VI) working solution was prepared by digestion of Pu(IV) in refluxing 1.0 M nitric acid for 8 h. The ^{239,240}Pu(VI) concentration was calculated based on the amount of Pu(IV) taken for oxidation, and visible spectroscopy indicates a valence purity of greater than 99%.

2.3. Spectrophotometric Titrations. UV−vis measurements were made on a 400-series charge-coupled device array spectrophotometer (Spectral Instruments Inc.) with a 200- to 950-nm scanning range. The solutions were held in PLASTIBRAND 1-cm cuvettes. The temperature was not controlled but monitored: the monitored temperature range is reported with the data. All solution spectra were referenced to a blank solution containing the supporting electrolyte (in most cases 1.0 M HNO_3). In titrations with U(VI), the optical absorbance from the bicyclic diamide was subtracted digitally at the data-processing stage.

Spectrophotometric titrations were performed by first introducing a single portion of the starting metal solution directly into the cuvette. The ligand then was introduced either by dissolving tiny aliquots of neat TMMA or by adding preweighed portions of solid **1a** directly into the cuvette. The increase in solution volume after each step of ligand addition and dissolution was estimated based on a calibration plot generated for each ligand in a separate experiment. Reliable data could not be obtained below 330 nm because the nitric acid solution itself absorbs strongly in this region. Equipment limitations restricted the upper range to 950 nm. The wide scanning range was used to monitor possible deviations from the initially adjusted valence state in the case of U(VI), Np(V), Pu(IV), and Pu(VI) during the spectrophotometric titration. The

(7) Bozhenko, E. I. In *Second International Symposium on Knowledge Acquisition, Representation and Processing (KARP-95)*; Auburn University: Auburn, AL, 1995; pp 10−13.
(8) Leggett, D. J. Stability Quotients from Absorbance Data. In *Computational Methods for the Determination of Formation Constants*; Leggett, D. J., Ed.; Plenum Press: New York, 1985; Chapter 6.
(9) Gilbertson, R. D.; Parks, B. W.; Hutchison, J. E.; Rapko, B. M.; Hay, B. P. *J. Org. Chem.* manuscript in preparation.
(10) Carnall, W. T. The Absorption and Fluorescence Spectra of Rare Earth Ions in Solution. In *Handbook on the Physics and Chemistry of Rare Earths*; Gschneider, K. A., Jr., Eyring, L., Eds.; North-Holland Publishing Company: Amsterdam, The Netherlands, 1979; Chapter 24.
(11) Yakovlev, G. N.; Kosyakov, V. N. In *Proceedings of the International Conference on the Peaceful Uses of Atomic Energy*; United Nations: New York, 1956; Vol. 7, pp 363−368.
(12) Schmieder, H.; Kuhn, E. *Chem.-Ing.-Tech.* **1972**, *44*, 104−111.

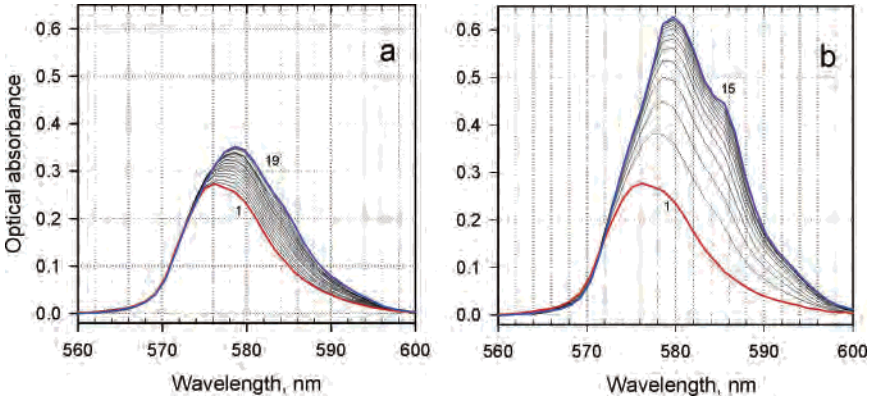

Figure 2. Spectrophotometric titration data for Nd(III) complexation with TMMA (a) and **1a** (b) in 1.0 M HNO_3. In both cases, the starting Nd concentration is 0.038 M (spectra 1). The ligand concentrations varied from 0.0475 to 0.904 M with TMMA (spectra 2−19) and from 0.051 to 0.855 M for **1a** (spectra 2−15).

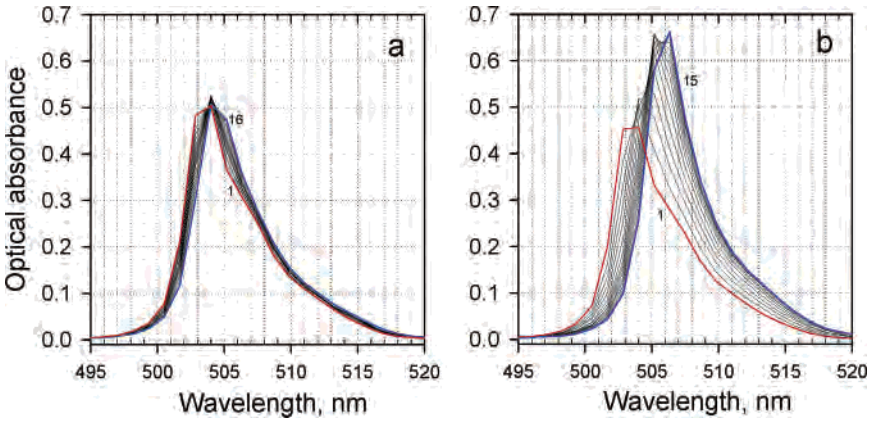

Figure 3. Spectrophotometric titration data for ^{243}Am(III) complexation with TMMA (a) and **1a** (b) in 1.0 M HNO_3. The starting Am concentrations are 1.79 mM and 1.58 mM (spectra **1a** and **1b**, respectively). The ligand concentrations varied from 0.048 to 0.844 M with TMMA (spectra 2−16) and from 0.0078 to 0.768 M for **1a** (spectra 2−15).

data-processing ranges were selected around the major absorption maxima of metal cations as follows: Nd(III) 560 to 600 nm; Am-(III) 490 to 520 nm; Pu(IV) 440 to 510 nm; Np(V) 600 to 660 nm; U(VI) 360 to 500 nm; Pu(VI) 810 to 860 nm.

2.4. Data Processing. Singular value decomposition analysis (SVD)[7] was employed to determine the number of spectrophotometrically distinct species in the optical absorbance spectral data sets collected during spectrophotometric titrations. It is based on a statistical analysis, free of any chemical model, and does not use any a priori assumptions of chemical nature; the analysis assumes only the validity of the Beer−Lambert law of optical absorbance for multicomponent mixtures.

The number of spectroscopically identifiable species determined by SVD analysis was used to choose a chemical model for the input file of the nonlinear spectra processing routine known as SQUAD. A modified version of the SQUAD code[8] was employed to refine the stability constants of the light-absorbing complexes of the 4f- and 5f-metal cations from the relevant spectral sets.

3. Results and Discussion

3.1. Results with the Trivalent f-Metal Cations Nd(III) and Am(III). Initial tests were done with Nd(III). A number of metal absorbance peaks in the visible range were examined with special focus on the hypersensitive absorbance band of Nd at 576 nm.[10] The results of this experiment yielded formation constants for both ligands with Nd(III) and played an important role in planning and executing the much more challenging experiment with radioactive ^{243}Am. Figures 2 and 3 show the results from spectrophotometric titrations of Nd(III) and Am(III) by the diamide ligands in 1.0 M HNO_3. In both cases, TMMA induces less pronounced spectral changes in the metal absorbance bands. SVD analysis indicates the formation of two, spectrophotometrically distinct, Nd-**1a** complexes and three, spectrophotometrically distinct, Am-**1a** complexes, whereas with TMMA, only one metal−ligand complex can be distinguished. The respective formation constants for both metals with both TMMA and **1a**, along with the spectral characteristics of the resolved species, are reported and discussed further below.

Next, a series of experiments was conducted with Nd(III) and both diamides at a constant ionic strength of 1.0 M but at three different acidities (0.01, 0.1, and 1.0 M). Each spectral data set was processed with a simple chemical model without assuming any impact from protonation of the ligands. In this analysis, if protons do actually compete with M^{3+} metal cation for the ligand, the concentration of free ligand in solution will be reduced compared to the values used to calculate an M−L formation constant. Any effective decrease in free ligand then should be manifested as a decrease in the calculated metal−ligand formation constants as the solution acidity increases. In Table 1, the impact of solution acidity on the conditional formation constants is summarized.

Table 1. Conditional Formation Constants of Nd(III) and Am(III) with **1a** and TMMA for Different Acidities at 1.0 M Ionic Strength and 23 ± 0.5 °C

		$\log\beta_{ij}$, Nd			$\log\beta_{ij}$, Am
complexant	species M_iL_j	0.01 M HNO_3	0.1 M HNO_3	1.0 M HNO_3	1.0 M HNO_3
1a	1:1	1.66 (0.04)	1.67(0.03)	1.50(0.02)	1.81(0.01)
	1:2	2.53(0.07)	2.51(0.04)	2.09(0.04)	2.91(0.02)
	1:3				3.07(0.04)
TMMA	1:1	−0.10 (0.01)	−0.33 (0.04)	−0.42 (0.04)	−0.17(0.05)

The data summarized in Table 1 show that for **1a**, there is no statistically significant effect from proton competition with the metal for the ligand at centi- and decimolar acidities, while for TMMA, such an effect is notable even at these low acid concentrations. On the other hand, over an acidity range of 0.1 M to 1.0 M, both ligands show a decrease in the calculated metal−ligand formation constants consistent with proton competition. Indeed, the apparent proton competition now is more significant for **1a** than with TMMA. If one assumes that there is no initial ligand protonation at the lowest examined acidity (0.01 M nitric acid) and that a 50% protonation of the ligand negatively shifts the apparent formation constant by $10^{0.3}$, it appears that 50% of the TMMA is protonated at 1.0 M acidity [$-0.42 - (-0.10) = -0.32$]. However, for **1a**, this effect is approximately twice less ($1.66 - 1.50 = 0.16$), or only 30% of **1a** is protonated at 1.0 M nitric acid.

An independent measurement of these ligand protonation constants by a separate spectrophotometric experiment involving acid titration of the ligand in the absence of metal was not attempted in $HNO_3/NaNO_3$ because of strong optical interference from nitrate. Instead, a spectrophotometric titration in the more optically transparent HCl/NaCl medium was tried. However, the spectral data led to poorly converging results and so were inconclusive.

A comparison between the results for Nd(III) and Am(III) reveals several interesting features. It is noteworthy that despite the close similarity of Nd(III) to Am(III) in terms of ionic radius,[13] both ligands show less affinity toward Nd(III) than to its 5f size-equivalent metal cation. This reduction in Nd(III) affinity is manifested in the systematic differences in the formation constants for the two ligands with these metals. In addition, Am(III) is able to accept a third ligand in the case of **1a**, while the same ligand with Nd forms only two observable complexes (all attempts to process Nd(III)-**1a** spectral sets assuming the presence of the 1:3 complex with **1a** failed). Finally, this difference is consistent with the relative extraction affinities for these two metals as reported previously.[14]

Another interesting result is that the difference at 1.0 M acidity between the log of the magnitudes for the first formation constant with the two ligands is remarkably consistent: 1.92 ± 0.05 for Nd(III) and 1.98 ± 0.05 for Am(III). We hypothesize that for higher complexes with trivalent f-elements, the same magnitude of difference should be expected for each subsequent step of complexation. Unfortunately, spectrophotometry cannot reliably measure formation constants with $\log\beta$ less than −0.7 [15] and, given the low value for the first formation constant of M(III) with TMMA coupled with the fact that the higher order stepwise formation constants will be even weaker, no spectral evidence for 1:2 and higher species could be detected in the M(III)−TMMA titration experiments. However, keeping in mind that the extraction stoichiometry of lanthanides (Eu) and actinides (Am) has been shown to be 1:3[6] (i.e., three molecules of extractant are bound to metal center), our data support the explanation that the approximately 1 million times enhancement in extraction efficiency of **1b** over acyclic tetraalkylmalonamides with trivalent metal cations can be ascribed to enhanced metal−ligand binding by the bicyclic diamide over acyclic malonamides.

3.2. Results with the Tetravalent Cation Pu(IV). During the spectrophotometric titrations with 8 mM Pu(IV), neither precipitation nor perturbations in the oxidation state of Pu(IV) were observed with either ligand. With **1a**, the most significant spectral changes observed with increasing ligand concentration were found in the region of the main Pu(IV) peak (a 476 → 497 nm shift, Figure 4b) and in the red part of the Pu(IV) spectrum (a 660 → 684 nm shift and a 2.4 times intensification of the absorption band). The spectral changes observed with TMMA were similar (less pronounced), but not identical to those observed with **1a**, and occurred only at much higher ligand-to-metal ratios (Figure 4a). An analysis of the number of species present, based on the singular value decomposition procedure,[7] advocated the presence of not less than four complexed species for the Pu(IV)-**1a** system and the presence of three major complexed species, with a possible (but minor) contribution from a fourth species in the TMMA-Pu(IV) system. The refined formation constants are presented and discussed in Table 2 (Section 3.6) and the respective spectral features of individual complexes are shown in Table 3 (Section 3.6).

3.3. Results with the Pentavalent Cation Np(V). Initial experiments during the spectrophotometric titration of Np(V) by **1a** in 1.0 M HNO_3 revealed that the pentavalent oxidation state of Np was not stable in the presence of this ligand. A fairly rapid transformation of Np(V) to a Np(IV)−ligand complex was observed over the time scale of hours as a progressive enhancement of the initially absent peak intensity at 732 nm, which is a 9-nm red shift from the major, 723-nm, peak of Np(IV) in 1.0 M HNO_3.[16] A reduction of the solution acidity to 0.1 M HNO_3, while keeping the ionic strength at 1.0 M with $NaNO_3$, helped to suppress metal

(13) David, F. *J. Less-Common Met.* **1986**, *121*, 27−42.
(14) Madic, C.; Hudson, M. J. *High-Level Liquid Waste Partitioning by Means of Completely Incinerable Extractants*; EC Report, 1998, EUR 18038 EN.
(15) Hartley, F. R.; Burgess, C.; Alcock, R. M. In *Solution Equilibria*; Ellis Horwood Ltd.: Chichester, U.K., 1980.
(16) Friedman, H. A.; Toth, L. M. *J. Inorg. Nucl. Chem.* **1980**, *42*, 1347−1349.

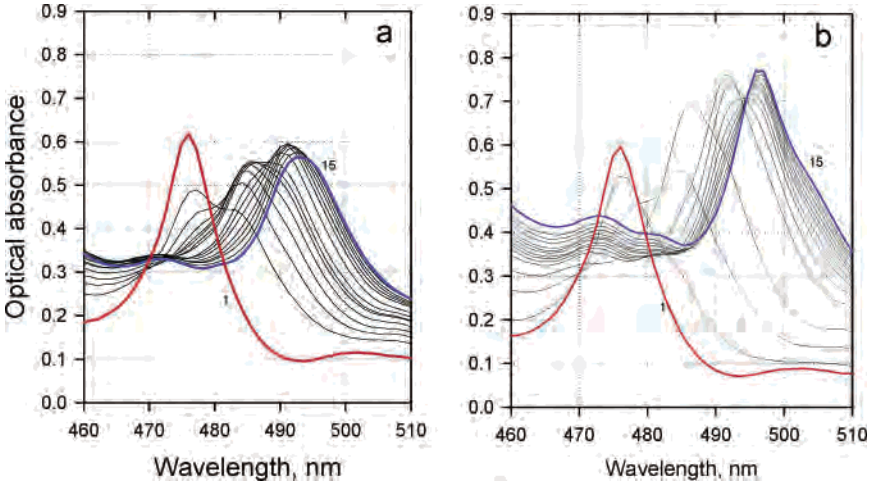

Figure 4. Spectrophotometric titration data for ^{239,240}Pu(IV) complexation with TMMA (a) and **1a** (b) in 1.0 M HNO_3. The starting Pu concentrations are 8.1 mM and 7.7 mM (spectra #**1a** and **1b**, respectively). The ligand concentrations varied from 0.0097 to 0.724 M with TMMA (spectra 2−15) and from 0.0026 to 0.629 M for **1a** (spectra 2−15).

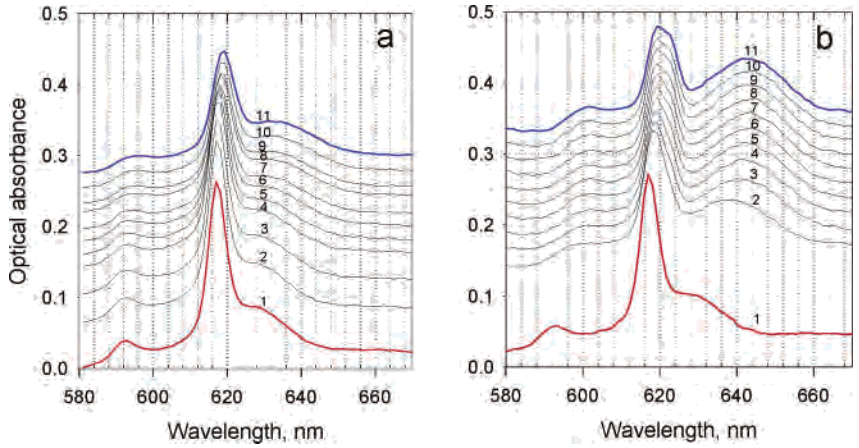

Figure 5. Spectrophotometric titration data for ^{237}Np(V) complexation with TMMA (a) and **1a** (b) in 0.1 M HNO_3/0.9 M $NaNO_3$. In both cases, the starting Np concentration is 12.7 mM (spectra 1). The ligand concentrations varied from 0.064 to 1.38 M with TMMA (spectra 2−11, offset for clarity) and from 0.066 to 0.696 M for **1a** (spectra 2−11, offset for clarity).

reduction, and Figure 5 shows the results of the spectrophotometric titration of Np(V) at this reduced acidity by TMMA and by **1a**. Again, as was noticed with Am(III) and Pu(IV), the preorganized ligand **1a** induces more pronounced changes with Np(V) compared to the acyclic malonamide. Refinement of the spectral data indicates two complexed species for Np(V) with **1a** but only one complex with TMMA. Table 3 (Section 3.6) shows the peak positions and molar absorptivities of the respective species; their formation constants are presented in Table 2 (Section 3.6). The magnitudes of the formation constants for Np(V) **1a** and Np(V)(**1a**)$_2$ are notably higher than the respective values for Am(III), while for TMMA the opposite is true. The TMMA results are more consistent with the general observation that AnO_2^+ species forms the weakest complexes among all other actinides.[17] It appears that preorganization of the malonamide functionality leads to an unexpected selective enhancement of the chelating effect with this monocharged dioxocation [$\log\beta_1^{\mathbf{1a}} - \log\beta_1^{\mathrm{TMMA}}$ = 2.22 − (−0.51) = 2.73 compared to that observed for Am(III) and Pu(IV)].

The preorganized diamide structure in **1a** offers not only preferential binding of Np(V) compared with trivalent actinides and lanthanides but also can act as a reductant to convert Np(V) to Np(IV) at higher acidity. Both these factors should facilitate Np extraction from acidic solution along with minor actinides by lipophilic analogues of **1a** when compared with acyclic diamides. However, to the best of our knowledge, no extraction measurements with conventional malonamide-based extractants have been reported in the literature for Np.

3.4. Results with the Hexavalent Cation U(VI). Both TMMA and **1a** induced significant spectral changes in the UO_2^{2+} spectrum, accompanied by a bathochromic shift and intensification of the absorption bands (Figure 6). Analysis of the spectral data sets indicates that **1a** again acts as a much stronger binding agent compared to TMMA. In neither case was spectral evidence found for the formation of higher M/L complexes (1:3 and 1:4 stoichiometry). Unlike Np(V) in 1.0 M nitric acid, U(VI) appears to be a redox stable cation when complexed with **1a** as judged by the lack of any measurable

(17) Ahrland, S. Solution Chemistry and Kinetics of Ionic Reactions. In *The Chemistry of the Actinide Elements*, 2nd ed.; Katz, J. J., Seaborg, G. T., Morss, L. R., Eds.; Chapman and Hall: New York, 1986; Vol. 2, Chapter 21.

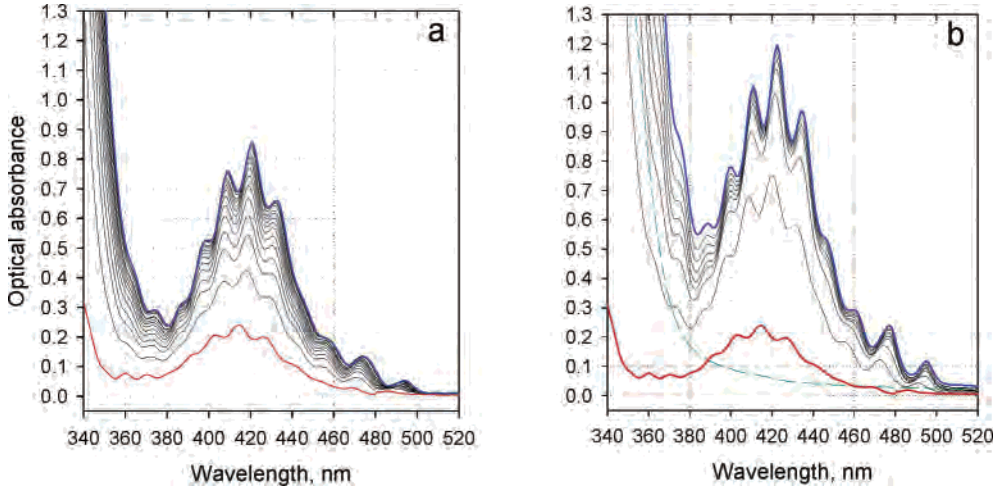

Figure 6. Spectrophotometric titration data for U(VI) complexation with TMMA (a) and **1a** (b) in 1.0 M HNO_3. In both cases, the starting U concentration is 29 mM (spectra 1). The ligands' concentrations varied from 0.048 to 0.843 M with TMMA (spectra 2−16) and from 0.025 to 0.415 M for **1a** (spectra 2−9). The dashed line shows the spectrum of **1a** at a concentration of 0.204 M.

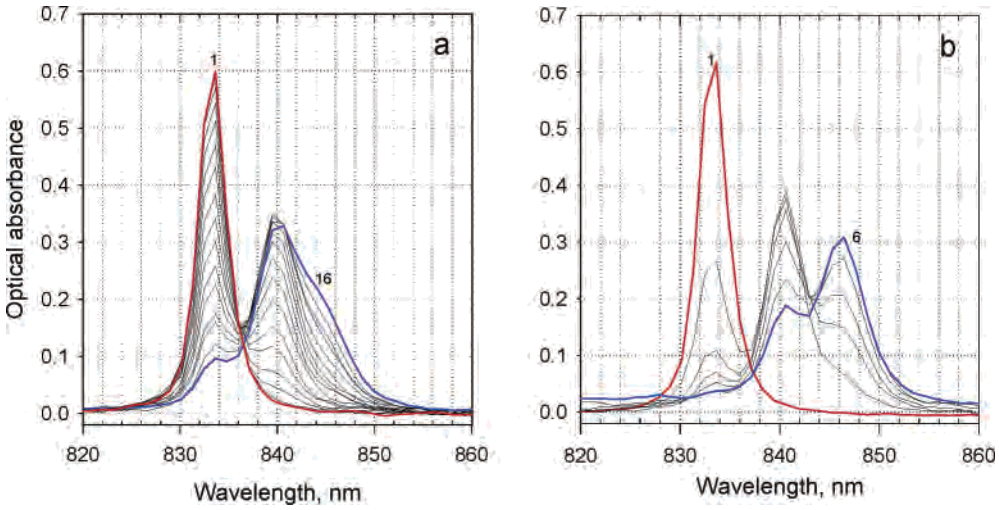

Figure 7. Spectrophotometric titration data for ^{239,240}Pu(VI) complexation with TMMA (a) and **1a** (b) in 1.0 M HNO_3. The starting Pu concentrations are 1.47 mM or 1.54 mM (spectra 1a and 1b, respectively). The ligand concentrations varied from 0.0092 to 1.31 M with TMMA (spectra 2−16) and from 0.0075 to 0.0758 M for **1a** (spectra 2−6).

optical absorbance in the 600−700-nm range where the major absorbance peak of U(IV) is located.[12]

3.5. Results with the Hexavalent Cation Pu(VI). Not only was the most intense and sharpest absorption peak of Pu(VI) at 833.6 nm[12] monitored for the expected complexation effects, but a wider range (330−950 nm) was examined to evaluate any possible changes in the oxidation state of the Pu. As was found with Pu(IV), **1a** induced prominent spectral changes in the visible spectrum with two, new, well-resolved peaks at 840.6 and 846.3 nm emerging even with the introduction of only a moderate excess of ligand (Figure 7b). However, after reaching a ligand-to-metal molar ratio of 80, further changes in the spectrum of hexavalent Pu were observed, with all three peaks of Pu(VI) gradually disappearing and a number of new spectral features emerging. In the visible range of the spectrum, the new major peak maxima were now at 497 and 684 nm. This new spectral signature clearly indicates the reduction of Pu(VI) to Pu(IV) in the presence of **1a**. A careful redox speciation analysis of the Pu(VI and IV) spectra also indicates that the Pu(VI) reduction is accompanied by the formation of Pu(V) (located as a weak spectral feature of a very low and variable intensity at 568 nm).[18] After accounting for the presence of Pu(IV) and Pu(V), the portion of the spectral set ascribed to Pu(VI) was processed by SQUAD; the respective formation constants refined from this analysis are shown in Table 2. In contrast to **1a**, the complexation of Pu(VI) with TMMA did not induce any redox reaction (even after an overnight contact time) and showed significantly weaker complexation effects, with the 1:2 complex seen not as a separate peak but only as a weak shoulder in the 842−846-nm range (Figure 7a).

3.6. Summary of Formation Constants and Spectral Features. Table 2 summarizes all the formation constants refined in the course of this project. The presented data reveal quantitatively the extent to which the preorganized diamide **1a** is a more efficient complexant than its conventional, acyclic counterpart TMMA.

(18) Cohen, D. *J. Inorg. Nucl. Chem.* **1961**, *18*, 211−218.

Table 2. Summary of the Conditional Overall Formation Constants of Am, Pu, Np, and U Complexes with **1a** and TMMA in 1.0 M HNO_3 at 23 ± 0.5 °C (Values in Brackets Represent One-Sigma Standard Deviations)

		$\log\beta_{ij}$				
complexant	species M_iL_j	Am(III)	Pu(IV)	Np(V)[a]	U(VI)	Pu(VI)
1a	1:1	1.81(0.01)	4.42 (0.08)	2.22(0.19)	2.85 (0.02)	2.36 (0.04)
	1:2	2.91(0.02)	7.95 (0.14)	3.21(0.23)	4.61 (0.05)	3.44 (0.07)
	1:3	3.07(0.04)	10.36 (0.1−)			
	1:4		11.48 (0.14)			
TMMA	1:1	−0.17(0.05)	2.56 (0.08)	−0.51(0.06)	1.00 (0.01)	0.44 (0.01)
	1:2		4.08 (0.11)		0.97 (0.03)	−0.03 (0.03)
	1:3		5.01 (0.14)			
	1:4		4.50 (0.38)			

[a] Measured in 0.1 M HNO_3/0.9 M $NaNO_3$ solution.

The Pu(IV) case is probably the most illustrative one in this respect because all four complexation steps were quantified with both ligands; the overall gain in binding strength at the final stage of complexation is found to be as high as 7 orders of magnitude. With TMMA, all four oxidation states of actinides follow a well-established order of affinity of 5f-element metal cations toward bidentate chelating agents: An(V) < An(III) < An(VI) < An(IV).[19] It appears that the preorganized diamide functionality somewhat modifies this order by making Np(V) a better coordinating metal center than Am(III). This is a very unusual observation, and a more extensive study directed at understanding the source for this change in the actinide binding sequence is indicated.

No quantification of complexation ability of TMMA on the second and further steps of complexation was performed with Am(III) and Np(V). Their presence cannot be detected in the spectral data sets, and it appears that the binding constants of these species are too low to form in appreciable yields under these experimental conditions.

All the formation constants refined in the course of this project must be considered conditional for two reasons. First, protonation of the ligands was not included in the formation-constant analysis. Second, all the experiments were performed at 1.0 M total nitrate concentration. Nitrate is known to be a weak complexing agent for An(III, V, and VI). LogK_1 has been reported as −0.26, −0.25, and −0.30 for Am(III), Np(V), and U(VI) at 1.0, 2.0, and 1.0 M ionic strength, respectively.[19] For Pu(IV), the existence of mono and dinitrato complexes at 2.0 M ionic strength has been reported with $\log K_1 = 0.51$ and $\log(K_1K_2) = 1.05$ for 2.0 M.[20] Even so, the effect of nitrate complexation was not included in the refinement that led to the reported formation constants.

The impact of nitrate complexation was evaluated qualitatively as follows. A speciation diagram generated based on the last two values at 1.0 M nitrate concentration indicates that only 6% of Pu(IV) would be present in solution as the nitrate-free species, with the remaining 94% being present either as $Pu(NO_3)_1^{3+}$ (22%) or $Pu(NO_3)_2^{2+}$ (72%). In reality, at a lower (1.0 M) ionic strength, the nitrate binding constants should be higher, and so the percentage of free Pu^{4+} is expected to be somewhat lower than 6%. An attempt to include nitrate complexation for Pu(IV) into the chemical model of its binding by **1a** and TMMA resulted in an increase of the respective formation constants by a factor of not lower than $10^{1.3}$. For U(VI) and Pu(VI), the nitrate complexation effect should be much less significant. Therefore, this qualitative accounting for the effect of nitrate makes the differences between the An(IV) and An(VI) formation constants even greater than is indicated from the results presented in Table 2.

It is of interest to compare the ligands' affinity toward the studied actinide metal cations, not through just the overall formation constants, but by comparing their stepwise changes, i.e., by looking at the $\log K^i_{\mathbf{1a}} - \log K^i_{\mathrm{TMMA}}$ difference at each complexation step ($i = 1, 2, 3, 4$). Such a differential plot is shown in Figure 8. One can see that for the first complexation step, the magnitude of the enhancement of **1a** over TMMA for tri-, tetra, and hexavalent actinides is remarkably uniform with the relative standard deviation not exceeding 3%. However, Np(V) clearly does not obey that regularity and represents a remarkable exception from the rest of the actinides. At present, we have no explanation why Np(V) behaves so differently from its AnO_2^{2+} structural analogues. For the second step of complexation, the data are more scattered, but again the average gain is similar to the one found at the first stage of complexation. This statistical interactinide comparison could not be performed for steps 3 and 4 because data are available only for Pu(IV).

All essential spectral data obtained by the deconvolution of spectral sets are summarized in Table 3. Comparison of the respective spectral signatures for the species of the same stoichiometry with the two complexants shows that, in most cases, the respective peak positions are identical or very close to each other, and peak intensities show a similar intensification trend as the complexation progresses. This can be seen most clearly from the Pu(IV), U(VI), and Pu(VI) data where both ligands form the same number of complexes. For Am(III) and Np(V), less data are available for such a comparison because with both of these metal cations, only 1:1 spectrophotometrically detectable complexes are present.

Again, the Np(V) case deserves special comment: not only does **1a** show a markedly higher preference to the metal cation in comparison with An(III, IV, and VI), but this preorganized ligand induces much more pronounced spectral changes in the 625−645-nm range (compare spectra 10 and

(19) Martell, A. E.; Smith, R. M. In *Critical Stability Constants*; Standard Reference DataBase 46, Version 6.0; National Institute of Standards, U.S. Dept. of Commerce: Gaithersburg, MD, 2001.
(20) Berg, J. M.; Veirs, D. K.; Vaughn, R. B.; Cisneros, M. R.; Smith, C. A. *Appli. Spectrosc.* **2000**, *54*, 812−823.

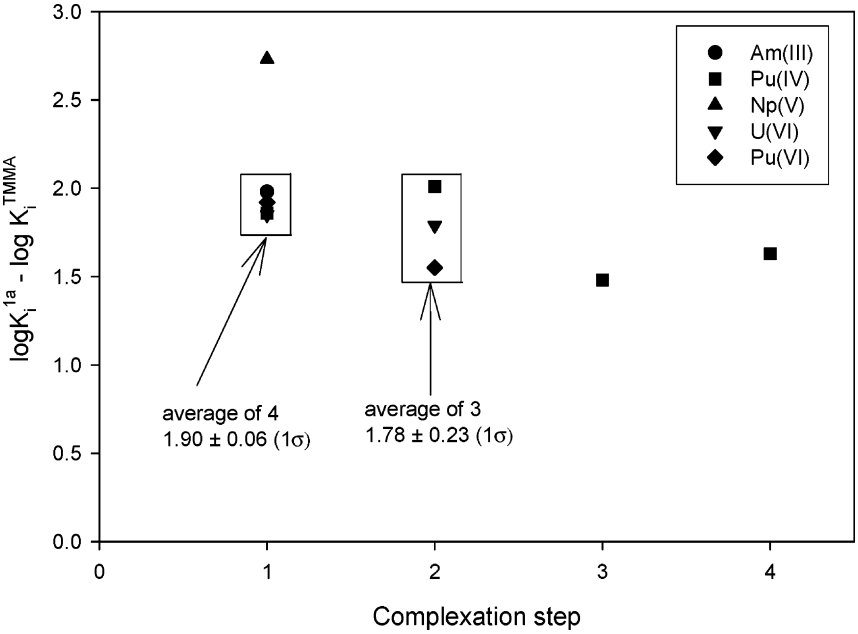

Figure 8. Comparison of stepwise formation constant between **1a** and TMMA for various oxidation states of actinide metal cations at each step of complexation.

Table 3. Molar Absorptivities and Maxima Positions of the Single-Component Actinide Complexes with Diamides Resolved by SQUAD

		molar absorptivity, M^{-1} $cm^{-1}{}_{wavelength,nm}$				
complexant	species M_iL_j	Am(III)	Pu(IV)	Np(V)	U(VI)	Pu(VI)
metal only, no ligand	1:0	$280_{503.4}$	$76_{476.0}$	$19.7_{616.9}$	$8.3_{414.1}$	$410_{833.6}$
1a	1:1	$386_{504.0}$	$77_{483.0}$	$19.8_{618.1}$	$34.0_{419.9}$	$420_{840.6}$
	1:2	$492_{505.2}$	$106_{486.5}$	$17.8_{621.6}$	$40.5_{422.3}$	$700_{846.5}$
	1:3	$563_{506.3}$	$113_{492.0}$			
	1:4		$102_{497.0}$			
TMMA	1:1	$432_{504.0}$	$68_{483.0}$	$27.8_{619.3}$	$31.9_{418.8}$	$460_{839.4}$
	1:2		$86_{486.5}$		$47.0_{422.3}$	$543_{844.1}$
	1:3		$82_{492.0}$			
	1:4		$107_{497.0}$			

3 in Figure 5a and b, respectively, for which the narrow peak at 617 nm shows the same degree of complexation). It would be desirable to extend the study of Np(V) complexation to diamides with a different degree of structural preorganization by extending the scannable spectral range to 1000 nm. This would allow inclusion of the major absorbance peak for Np(V) at 981 nm ($\epsilon = 395$ $M^{-1}cm^{-1}$ [16]) and so allow for additional spectral analysis.

3.7. Analysis of the Redox Behavior of Pu(VI) and Np-(V) in the Presence of 1a and TMMA. The remarkable ability of the bicyclic diamide to promote reduction of the transuranium dioxocations Pu(VI) and Np(V) in 1.0 M nitric acid solution deserves additional comment.

As previously mentioned, Pu(VI) undergoes reduction in the presence of ~80-fold excess of the ligand to the tetravalent state. The rate of reduction is relatively fast after an induction period (~40 min after the first addition of the ligand); the reduction appears complete within a few hours after introducing the last portion of ligand. The formal redox potential of the Pu(VI)/Pu(IV) couple at pH = 0 is known to be +1.043 V;[21] in other words, Pu(VI) acts as a mild oxidizing agent in acidic solution. Pu(VI) is known to be reduced by a number of inorganic and a few organic agents,[22] although, to our knowledge, the reduction of Pu(VI) by malonamides has not been described previously. We believe that the drastic difference in redox activity between **1a** and TMMA can be attributed to the effect of complex formation on the electrochemical potential of the Pu(VI)/Pu(IV) couple. As described above, both Pu(IV) and Pu(VI) form complexes with **1a** and TMMA; however, not only is the complex formation much stronger for **1a** than for TMMA, but also for both ligands, the lower oxidation state Pu(IV) forms much stronger complexes than does the more oxidized Pu(VI).

The magnitude of the change in the electrochemical potential induced by the complex formation from the simple aquo ions can be described by the modified Nernst equation[23] (see below)

$$E = E_0' + \frac{RT}{nF}\ln\frac{1 + \beta_1^{red}[L] + \beta_2^{red}[L]^2 + ... + \beta_p^{red}[L]^p}{1 + \beta_1^{ox}[L] + \beta_2^{ox}[L]^2 + ... + \beta_q{}^{ox}[L]^q} + \frac{RT}{nF}\ln\frac{C_{M_{Ox}}}{C_{M_{Red}}} \quad (1)$$

where E_0' is formal potential of the Pu(VI)/Pu(IV) redox couple; β_i^{red} and β_i^{ox} denote the overall formation constants of Pu(IV) and Pu(VI), respectively, at the *i*-th step of complexation ($i = 4$ and $i = 2$ for the tetra- and hexavalent Pu respectively); $[L]$ denotes the complexing agent's concentration in solution; and $C_{M_{Ox}}$ and $C_{M_{Red}}$ are total solution concentrations of Pu(VI) and Pu(IV). At room temperature

(21) Coleman, G. H. In *The Radiochemistry of Plutonium*; National Academy of Sciences/U.S. Atomic Energy Commission Report NAS-NS-3058; Lawrence Radiation Laboratory, University of California: Livermore, CA, 1965.
(22) Newton, T. W. Redox Reactions of Plutonium Ions in Aqueous Solutions. In *Advances in Plutonium Chemistry 1967−2000*; Hoffman, D. C., Ed.; American Nuclear Society: La Grange Park, IL, 2002; Chapter 3.
(23) Laitinen, H. A. In *Chemical Analysis*; McGraw-Hill Series in Advanced Chemistry; McGraw-Hill: New York, 1960; Chapter 15.

Table 4. Effect of Complexation of Pu(IV) and Pu(IV) on the Shift of the Formal Electrochemical Potential of the Pu(VI)/Pu(IV) Couple in the Presence of **1a** and TMMA (Columns 2, 4, and 6); Np(V)/Np(IV) Calculations Are Added for Comparison (Columns 3, 5, and 7; see Section 3.7 for More Details)

	complexation term in eq 1, mV				**1a**−TMMA difference in complexation term, mV	
	1a		TMMA			
[L], M	Pu(VI/IV)	Np(V/IV)	Pu(VI/IV)	Np(V/IV)	Pu(VI/IV)	Np(V/IV)
0.01	120	246	23	46	97	199
0.03	149	306	41	85	108	222
0.1	181	372	69	146	111	226
0.2	199	410	89	191	110	219
0.4	217	447	109	242	108	205
0.6	228	469	120	274	107	195
0.8	235	484	129	298	107	186

and for the two-electron reaction ($PuO_2^{2+} + 4H^+ + 2e^- = Pu^{4+} + 2H_2O$), the numerical value of the RT/nF term is approximately 0.03 V.

For ligand concentrations in the millimolar range or higher, the first logarithmic term in eq 1 rapidly becomes large enough to produce a significant positive addition to E_0'. The magnitude of the change can be calculated using the measured formation constants for any desired concentration of ligand. Table 4 shows the results of such calculations for **1a** and TMMA.

As can be seen from an analysis of the data shown in the 2nd and 4th columns, both ligands positively shift the formal potential of the Pu(VI)/Pu(IV) couple, and the magnitude of this shift increases as the concentration of diamide increases. Interestingly, a TMMA concentration of 0.6 M is required to produce the same positive shift as a 0.01 M concentration of **1a**. Evidently, based on the absence of reduction observed during the Pu(VI)−TMMA test, a positive shift of ~130 mV is insufficient for Pu(VI) reduction. However, it must be noted that this conclusion assumes that the oxidized species has either the same or similar reduction potential in both tests. It seems likely that in both cases the ligand is acting as the reductant; however, the oxidation potentials for either TMMA or **1a** are unknown. At equal ligand concentrations, **1a** induces an ~110 mV more positive shift compared to TMMA (column 6). For the two electron processes of Pu(VI) to Pu(IV) reduction, under otherwise identical conditions, this 110-mV difference results in a calculated $10^{(110/30)} = 10^{3.66}$ times difference in the $C_{Pu(VI)}/C_{Pu(IV)}$ ratio between TMMA and **1a**. If one assumes that at a 0.1 M concentration of TMMA, the Pu(VI) retains its initial valence purity of 99%, then the same concentration of **1a** would lower the concentration of Pu(VI) by almost 4 orders of magnitude. This estimate is consistent with the experimental observation of practically complete reduction of Pu(VI) in the ~0.08 M solution of **1a** present at the conclusion of testing.

The formal redox potential of the Np(V)/Np(IV) couple at pH = 0 in a noncomplexing medium is +0.739 V.[24] Unlike the Pu(VI) → Pu(IV) reaction, the reduction of Np(V) to its tetravalent state is a one-electron process: $NpO_2^+ + 4H^+ + e^- = Np^{4+} + 2H_2O$. From inspection of the half reactions for Pu(VI) and Np(V) reduction, one can observe that the reaction potential for Np(V) reduction is twice as sensitive to pH as the Pu(VI)/Pu(IV) couple. Indeed, by reducing the solution acidity from 1.0 to 0.1 M, one can calculate a decrease in the Np(V) reduction potential of $0.059 \times 4 = 0.239$ V. This significant decrease explains the experimental observation that a reduction in acidity helped to preserve Np in the pentavalent state during the course of titration by **1a** at a 0.1 M acid concentration. In 1.0 M nitric acid, however, the introduction of **1a** initiates reduction almost immediately. The observed reduction rate is somewhat slower than that observed for Pu(VI), with complete Np(V) → Np(IV) conversion taking place over several days.

Although Np(IV) formation constants with **1a** and TMMA were not measured in the course of this project, they should be reasonably well approximated by their respective Pu(IV) constants. This assumption allows the relevant complexation term to be calculated for the Np(V)/Np(IV) couple. Table 4 (columns 3, 5, and 7) shows how the extent of complexation of Np(V) and Np(IV) can positively shift the formal electrochemical potential of the Np(V)/Np(IV) couple as a function of ligand concentration for both **1a** and TMMA. Again, due to the one-electron character of this reduction, the magnitude of this positive shift appears to be about 2 times higher than that for the Pu(VI) reduction. Therefore, despite a notably less positive value of electrochemical potential of the Np(V)/Np(IV) couple [+0.739 V vs +1.043 V for Pu(VI/Pu(IV)], the presence of **1a** shifts the reduction potential to a value of approximately +1.15 to +1.20 V, which in turn makes Np(V) just as potent an oxidizer as Pu(VI).

Conclusions

In conclusion, applying UV−vis spectroscopy to the study of binding of actinides with the bicyclic diamide **1a** and the acyclic malonamide TMMA in acidic aqueous solution has allowed quantification of the binding constants for both bicyclic and acyclic diamide ligands with Am(III), Pu(IV), Np(V), Pu(VI), and U(VI). The results support the assumption in our earlier reports[5,6] that the source of the enhancement of +3 f-element extraction by **1b** over acyclic malonamides is due to an enhancement in the effectiveness of actinide complexation for the bicyclic diamide over similar, but acyclic, diamide agents. Other significant findings from this study include the following: (i) Both the Nd(III) and Am(III) data show preferential binding by **1a** in comparison with TMMA by a factor of $10^{(1.95\pm0.05)}$ for the first step of complex formation. (ii) The alternation of the diamide structure from acyclic to bicyclic increased the overall formation constants with Pu(IV) by as much as 7 orders of magnitude. (iii) The bicyclic diamide **1a** binds Np(V) more efficiently than Am(III), whereas with the acyclic diamide TMMA the opposite effect is observed. (iv) A comparison of An(VI)-ligand binding affinities reveals an enhanced binding to U(VI) versus Pu(VI) for the both ligands. (v) In the presence of Np(V) or Pu(VI), but not U(VI), the bicyclic diamide at 1.0 M acidity triggers the

(24) Burney, G. A.; Harbour, R. M. In *The Radiochemistry of Neptunium*; Report NAS-NS-3060; National Academy of Sciences, U.S. Atomic Energy Commission: 1974.

reduction of Np(V) to Np(IV) and Pu(VI) to Pu(IV). (vi) The nature of this unique redox activity of preorganized diamide as opposed to its acyclic analogue is associated with the effect of complexation on the positive shift of formal potentials of the Np(V)/Np(IV) and Pu(VI)/Pu(IV) couples. (vii) No significant change in the Nd(III)/Am(III) selectivity by **1a** versus TMMA was observed.

Acknowledgment. We gratefully acknowledge support of this work by the Environmental Technology Directorate at the Pacific Northwest National Laboratory (PNNL), by the Environmental Management Sciences Program of the Office of Science, U.S. Department of Energy (DOE), and by the National Science Foundation. The research was performed at PNNL, operated by Battelle for DOE under Contract DE-AC06-76RL01830, and at the University of Oregon.

IC049377M